24th International Conference on Renewable Energies and Power Quality (ICREPQ'26)
Santander (Spain), 10th to 12th June 2026
ISBN-13: 978-84-09-82044-3

System Rigidity: A Comprehensive Approach to Enhancing Power System Stability

I. Vokony[1]

[1] Department of Electric Power Engineering
Budapest University of Technology and Economics
Műegyetem rkp. 3., H-1111 Budapest, Hungary. vokony.istvan@vik.bme.hu

Abstract. The shift toward renewable-dominated power systems has significantly reduced inertia, challenging traditional stability metrics. This paper introduces system rigidity as a unified measure capturing frequency, voltage, and angle stability in low-inertia grids. A Rigidity Response Threshold (RRT) is defined as the maximum disturbance a system can endure without instability, derived using a Lyapunov-based framework. Validation through field tests on the Fót microgrid – including pump motor switching and PV disconnection – confirms that system rigidity aligns with known stability boundaries and outperforms inertia- or RoCoF-based indicators in sensitivity. The proposed rigidity metric and RRT offer operators a holistic tool to assess and enhance stability, supporting the deployment of synthetic inertia, fast frequency response, and advanced control strategies for future resilient power systems.

Key words. frequency stability, low-inertia systems, renewable energy integration, synthetic inertia, system rigidity

1. Introduction

Modern power systems are increasingly dominated by renewable and converter-based resources, which reduce system inertia and make stability more difficult to assess with traditional metrics. Recent large-scale disturbances have highlighted the vulnerability of low-inertia systems and the limitations of conventional indicators developed for synchronous generation-dominated grids.

System rigidity is proposed as a response to this challenge, offering an integrative measure of a power system's ability to withstand disturbances while maintaining acceptable operation [1]. Unlike conventional approaches that treat angle, frequency, and voltage stability separately, system rigidity combines these aspects within a single framework. This concept is quantified through the Rigidity Response Threshold (RRT), which defines the maximum disturbance that can be tolerated without loss of stable operation. In this way, RRT addresses limitations of traditional metrics such as critical clearing time or frequency nadir in low-inertia environments [2].

The remainder of the paper is organized as follows. Section 2 reviews the relevant background and related work. Section 3 introduces the theoretical framework of system rigidity. Section 4 presents the mathematical formulation of the RRT. Section 5 outlines the validation methodology. Section 6 describes the Fót microgrid field test and its results. Section 7 discusses the main findings, and Section 8 concludes the paper.

2. Literature review

A. Impact of low inertia on stability

Traditional power system stability has long relied on the buffering effect of synchronous machine inertia. The kinetic energy in large generators slows down frequency changes, aiding transient stability after disturbances. However, with renewable energy sources (RES) like wind and solar largely interfaced via inverters (which contribute virtually no physical inertia), modern grids experience much faster frequency drops for a given disturbance size compared to traditional systems [3]. Operators have observed higher rates of change of frequency (RoCoF) and deeper frequency nadirs in low-inertia conditions. For instance, following the 2021 CESA event mentioned above, frequency deviations approached stability limits within seconds – behavior that would have been less extreme in a high-inertia system. Reduced inertia also affects voltage and oscillatory stability, as converter-dominated systems lack the natural damping and overload capabilities of synchronous machines. These challenges necessitate rethinking stability criteria and tools.

B. Advances in stability enhancement

In response to these challenges, researchers and grid operators have proposed a range of innovative strategies. Key developments in the literature include:

- *Lyapunov-based analysis:* Lyapunov-based methods provide analytical stability criteria and energy-margin estimates, enabling the assessment of stability regions and critical clearing times without relying solely on time-domain simulations. [5]
- *Synthetic inertia:* Synthetic inertia enables converter-based resources to emulate inertial response during disturbances, thereby reducing frequency excursions and limiting RoCoF in low-inertia systems. [7]

- *Fast Frequency Control and energy storage:* Fast frequency control provided by energy storage systems, particularly BESS, enhances frequency stability and damping through rapid active power support following disturbances. [8]
- *Advanced control algorithms:* Adaptive and machine learning-based control strategies offer promising solutions for managing the complex dynamics of inverter-dominated systems, although this area remains in an early stage of development.
- *Bifurcation analysis:* Bifurcation analysis is useful for identifying operating conditions close to oscillatory instability or voltage collapse in systems with high renewable penetration. [9]
- *Hybrid simulation tools*: Hybrid EMT–RMS simulation approaches provide more accurate representations of fast transients and protection-related phenomena in converter-dominated power systems than RMS simulations alone. [10].

Several recent review studies synthesize these advances. For example, Milano et al. (2018) outline the foundations and open challenges of low-inertia systems, calling for new stability metrics beyond traditional ones [12]. Taczi et al. (2022) similarly emphasize that with high non-synchronous generation, traditional stability classifications must be extended [13]. They also highlight the need for unified metrics (such as the system rigidity proposed in this work) to ensure long-term security of supply.

This literature context underlines the contribution of system rigidity: it builds upon the above methods by providing a single cohesive measure of how "stiff" or resilient a power system is against disturbances.

In summary, while numerous techniques address specific facets of stability, a gap remains for a unified stability quantification in low-inertia grids. The concept of system rigidity is introduced to fill this gap, synthesizing insights from prior work into a comprehensive stability framework.

3. Theoretical framework

A. Concept of system rigidity

System rigidity is defined as the capacity of a power system to resist destabilizing disturbances and maintain stable operation within acceptable bounds. Formally, a rigid system remains near its equilibrium (within predefined small deviations) for any disturbance up to a certain critical magnitude. Beyond this point, even a slightly larger disturbance causes the system to exhibit large deviations or instability (losing synchronism, large voltage swings, etc.). This critical disturbance level is captured by the Rigidity Response Threshold (RRT). A high RRT value indicates a very rigid (robust) system that can tolerate large disturbances, whereas a low RRT signifies a fragile system nearing instability. Unlike traditional stability margins that are often phenomenon-specific (e.g., frequency nadir or critical clearing time), RRT provides a unified margin applicable across frequency, voltage, and angle domains.

B. Lyapunov-based stability analysis

To establish a rigorous foundation for system rigidity, we employ a Lyapunov-based approach Lyapunov's direct method offers a way to assess stability by constructing an energy-like function for the system. In this work, a composite Lyapunov function $\boldsymbol{V(x)}$ is formulated to represent the system's kinetic and potential energy, accounting for both frequency deviations and voltage variations in the network [5]. The equilibrium point (operating point) of the system is taken as the origin in this Lyapunov analysis.

$$\dot{x}(t)=f(x(t),p)+\eta(t)$$

Stability is guaranteed if $\boldsymbol{V(x)}$ remains positive definite and its time derivative $\boldsymbol{\dot{V}(x)}$ is negative definite (or at least negative semi-definite) in a region around the equilibrium. Using this framework, the RRT can be interpreted as the boundary of the region of attraction in the state space: it is related to the largest disturbance energy (or size) for which a valid Lyapunov function $\boldsymbol{V(x)}$ indicates the system will return to equilibrium.

We derive conditions for stability in terms of system parameters by analyzing $\boldsymbol{\dot{V}(x)}$. For example, consider a simplified system with state variables capturing rotor angle/frequency and voltage magnitudes. A candidate Lyapunov function might include terms like kinetic energy ($\sim\boldsymbol{\Delta\omega^2}$) and reactive energy stored in voltage deviations. The RRT corresponds to the maximum perturbation $\boldsymbol{|\eta(t)|}$ such that $\boldsymbol{V(x)}$ stays within a certain bound $\boldsymbol{\varepsilon}$ for all $\boldsymbol{t > t_0}$, ensuring the state remains in the stability region.

Mathematically, we can express this concept as an inequality constraint on the initial disturbance input to the system:

$$\boldsymbol{RRT = \max\{|\eta| : |z(t) - z^*| < \varepsilon, \forall t > t_0\}} \qquad (1)$$

where $\boldsymbol{z(t)}$ is the system state trajectory, $\boldsymbol{z^*}$ is the equilibrium state, $\boldsymbol{\eta}$ represents an external disturbance (initial perturbation or injection), and $\boldsymbol{\varepsilon}$ is a small allowable deviation.

In words, equation (1) defines RRT as the largest disturbance norm for which the system's state deviation $\boldsymbol{|z(t) - z^*|}$ remains bounded by $\boldsymbol{\varepsilon}$ at all times after the disturbance. If a disturbance exceeds this threshold, the Lyapunov function can no longer be assured to decrease, and the system may transition to a different (potentially unstable) equilibrium or diverging condition. Thus, RRT delineates the stability boundary in a Lyapunov sense.

C. Unified stability criteria

The Lyapunov-based formulation allows us to incorporate multiple stability aspects. Frequency stability enters via the kinetic energy term in $\boldsymbol{V(x)}$, voltage stability via potential energy terms (e.g., deviation of bus voltages), and rotor/angle stability via relative angle terms. By including inverter control dynamics in the model, the

Lyapunov analysis also accounts for high-bandwidth control actions.

The derived stability conditions relate directly to physical parameters: for instance, greater system inertia (including emulated inertia from inverters) tends to enlarge the stability region, increasing RRT. Stronger voltage support (e.g., fast reactive power control) also expands the stability region by mitigating voltage dips during disturbances. Fast-acting controls and proper coordination can further improve the Lyapunov stability margin by quickly counteracting disturbances, though poorly tuned controls might reduce the margin due to interactions.

The theoretical framework thus provides insight into which factors contribute to system rigidity. In summary, the key contributors to a rigid system include:

- *Inertia (physical and synthetic):* Higher inertia improves disturbance tolerance by slowing frequency deviations and generally increasing the RRT.
- *Voltage support and reactive power:* Fast reactive support strengthens voltage stability and increases the disturbance level the system can withstand.
- *Dynamic control responsiveness:* Fast control actions improve rigidity by rapidly compensating for imbalances, provided they are properly coordinated.
- *Network topology and control coordination:* Strong interconnection and coordinated controls enhance disturbance damping, whereas weak links and poor coordination reduce rigidity.

This theoretical foundation establishes system rigidity as a measurable, calculable metric. By combining Lyapunov analysis with practical system parameters, we obtain an analytic handle on stability that is suited to modern grids. In the next section, we translate this concept into a concrete formulation for RRT and outline how it can be computed and validated.

4. Mathematical Formulation of RRT

To quantify system rigidity, we formally define the Rigidity Response Threshold (RRT) based on system dynamics. RRT is the critical disturbance magnitude below which the system can absorb the perturbation and remain stable. If the disturbance exceeds RRT, the system's response becomes non-linear and transitions towards instability. Using the Lyapunov-based definition, RRT can be determined by finding the boundary of the stability region in terms of disturbance size (as in Equation 1). In practical terms, one can compute RRT through simulation or analytical estimation by gradually increasing the disturbance until the system just fails to recover to its pre-disturbance state.

From a mathematical perspective, consider a system modelled by a set of differential–algebraic equations (DAEs) representing generator dynamics, inverter controls, network power flows, etc. Let $\boldsymbol{x}(\boldsymbol{t})$ be the state vector (angles, speeds, voltages, etc.) and $\boldsymbol{x}^*$ the nominal equilibrium. We introduce a disturbance at time $\boldsymbol{t_0}$ (for example, a load step increase or generation trip) represented by a vector $\boldsymbol{\eta}$. The post-disturbance trajectory $\boldsymbol{x}(\boldsymbol{t})$ will either remain in a stable neighborhood of $\boldsymbol{x}^*$ or diverge/oscillate.

We can define RRT in terms of the system's region of attraction: essentially, RRT corresponds to the size of the largest disturbance $|\boldsymbol{\eta}|$ such that x(t) stays within the region of attraction of $\boldsymbol{x}^*$**.** This aligns with the Lyapunov characterization that there exists a Lyapunov function $\boldsymbol{V}(\boldsymbol{x})$ decreasing to 0 for all $\boldsymbol{x}$ within that region.

In practice, to determine RRT, we perform the following steps:

1) Analytical estimation
2) Incremental disturbance simulations
3) Probabilistic analysis
4) Verification of the RRT criterion

An *analytical estimation* can first be used to derive conditions for stability using a Lyapunov function or energy method. For instance, one might obtain an inequality of the form

$$|\boldsymbol{\eta}| < \Delta_{\boldsymbol{MAX}}\ (\boldsymbol{H}, \boldsymbol{D}, \boldsymbol{K}) \tag{2}$$

where $\Delta_{\boldsymbol{MAX}}$ is a function of system inertia $\boldsymbol{H}$, damping $\boldsymbol{D}$, control gains $\boldsymbol{K}$, etc., describing the maximum perturbation energy tolerable. This provides an initial estimate of RRT in terms of system parameters.

This estimate can then be refined through *incremental disturbance simulations* using a detailed dynamic model of the system, apply disturbances of increasing magnitude in a simulated environment. This can be done via time-domain simulation tools (RMS or EMT). Starting from a small disturbance and gradually raising its size, identify the point at which the system no longer returns to steady state (e.g., voltage collapse or frequency instability occurs). That disturbance level is taken as the RRT from simulation. Simulations should cover various disturbance types (load changes, generation loss, faults) to evaluate different facets of rigidity.

A further step is *probabilistic analysis*, which recognize that real-world disturbances and system conditions vary. Perform Monte Carlo simulations or parameter sensitivity studies by varying system conditions (load level, generation dispatch, control settings, etc.) and repeating the disturbance test. This yields a distribution of "failure points". The RRT can then be treated statistically, for example, defining a threshold that the system can tolerate with 95% confidence. This step adds a probabilistic robustness aspect to the RRT metric.

Finally, *verification of the RRT criterion* is achieved by comparing the simulation-identified RRT with analytical predictions. If discrepancies exist, refine the model or Lyapunov function. Often, unmodeled dynamics or control delays can cause differences. The process may iterate: update the theoretical model to include these effects and recompute RRT until analysis and simulation align within an acceptable tolerance.

The outcome of this formulation process is a validated value (or range) for the RRT for the given system. A higher RRT value indicates a more robust system, which can handle larger disturbances without instability. Conversely, a small RRT warns that even moderate disturbances could precipitate instability, signaling a need for system reinforcement or control enhancements.

Notably, RRT inherently integrates multiple stability modes; for example, if voltage instability is the first to occur for a certain disturbance size, it will manifest in the RRT determination even if frequency remains within limits. This makes RRT a comprehensive indicator of the "weakest link" in system stability for a given configuration.

By calculating RRT under different scenarios, operators can also gauge the effectiveness of stability improvements. For instance, adding a new BESS or tuning an inverter controller will change the RRT. In simulations presented in prior work, adding synthetic inertia or reactive support clearly increased the RRT, quantifying the benefit of those measures. A 50% reduction in physical inertia was found to reduce RRT by about 30%, illustrating the sensitivity of the stability margin to inertia. Meanwhile, combining fast frequency control with dynamic voltage support provided the greatest boost to RRT, underlining the importance of an integrated approach to stability.

These findings reinforce that RRT is a meaningful measure of system strength, and improvements in RRT correspond to intuitively stronger stability as observed in simulations.

With the RRT formulation in place, the next step is to validate the concept and methodology through practical testing.

5. Simulation and Validation Methology

To thoroughly evaluate the system rigidity concept and the RRT metric, we adopted a multi-pronged validation approach combining simulation studies with experimental field measurements. The methodology can be summarized as follows:

- *Detailed dynamic simulations:* RMS and EMT simulations were performed on low-inertia system models representing the Fót microgrid in order to identify the RRT under disturbances of increasing magnitude and to verify consistency with the Lyapunov-based stability interpretation. [16]
- *Laboratory testing:* Preliminary laboratory or RTDS-based tests were used to reproduce representative disturbances under controlled conditions, supporting the validation of measurement methods, control settings, and model assumptions before field deployment.
- *Field measurement campaign:* The main experimental validation was conducted at the Fót microgrid using PMU devices and fast data loggers installed at critical locations to record voltage, frequency, and power-flow transients during controlled disturbance events.
- *Data analysis and RRT validation:* The measured field responses were compared with the predicted rigidity threshold, showing stable recovery in all tested cases and supporting further refinement of the simulation model based on observed deviations.

By using this comprehensive validation methodology, we ensure that the proposed system rigidity metric is credible for real power systems.

6. Field test description and results

To demonstrate the unified stability metric in a real-world setting, a field measurement campaign was executed at the Fót microgrid test site. Fót microgrid is a small-scale, distribution-level system equipped with a mix of generation and loads, making it representative of a low-inertia network segment. The site includes two solar photovoltaic arrays (35 kW installed on a large barn and 23 kW on an office building), a Battery Energy Storage System (BESS), a 22 kW electric vehicle (EV) fast charger, and an industrial water pump among other loads. The microgrid is connected to the main utility grid through a transformer but can be operated in island mode for testing purposes.

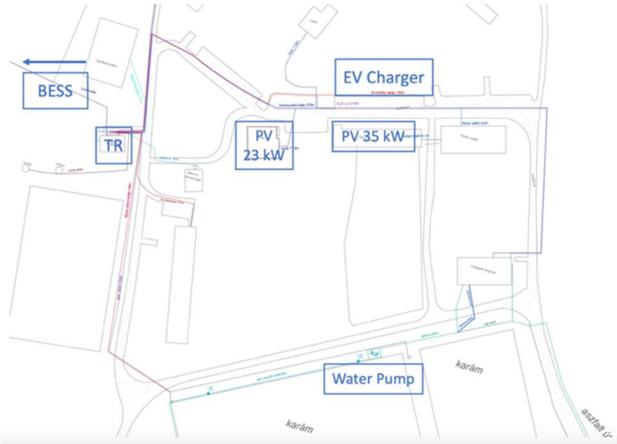

Fig. 1 Fót Microgrid layout

A. Measurement setup

For the field tests, high-precision measurement units were installed at critical nodes of the microgrid, including: (i) the main transformer (point of common coupling, PCC), (ii) the PV inverter outputs for the two solar plants, and (iii) the pump motor supply line.

Each unit recorded three-phase voltages and currents, allowing derivation of frequency (from voltage waveforms) and active/reactive power flows. The sampling rate was chosen to capture sub-second transients: PMU devices provided time-synchronized phasor data at 50 frames per second, and parallel waveform recorders captured detailed waveforms in the kHz range for event analysis. A GPS time reference ensured that all measurements could be aligned for analysis.

The microgrid was prepared in a stable operating condition prior to tests, with the BESS in a grid-forming control mode to regulate voltage and frequency, which is especially important when islanded from the main grid.

B. Disturbance scenario

We devised a worst-case (but controlled) disturbance to challenge the system's stability margin: a simultaneous large load increase and generation loss. At a scheduled time, the water pump motor was started (switched on) while almost concurrently the larger PV array (35 kW at the barn) was tripped offline (disconnected), effectively removing a significant generation source.

This combined disturbance, referred to as the "pump-on + PV-off" event, represents a sudden swing from the microgrid exporting solar power to the grid to suddenly drawing power to feed a motor load. According to prior simulations, this event was expected to be among the most severe transients for the system, potentially approaching the RRT.

The timing was coordinated such that the pump motor's inrush current and the PV inverter's disconnection overlapped, maximizing the impact. In the particular test run, the event was initiated at 00:40 (hh:mm:ss) in the recording. After approximately one minute of operation under this perturbed condition, the sequence was reversed: the PV inverter was reconnected and the pump was turned off at 01:44, allowing the system to return to its original state. This provided a full cycle of disturbance and recovery for analysis.

C. Observed system response

The Fót microgrid's response to the pump and PV disturbance was recorded by all measurement units.

At the moment of the disturbance (t=00:40), a sharp voltage drop was observed, most prominently at the pump's connection point and the nearby distribution bus. The voltage at the pump bus dipped by roughly 8–10% immediately when the motor started, indicating the effect of the inrush current and sudden loading. The main PCC bus and the barn's PV bus (which went offline) experienced a smaller but noticeable voltage sag of a few percent.

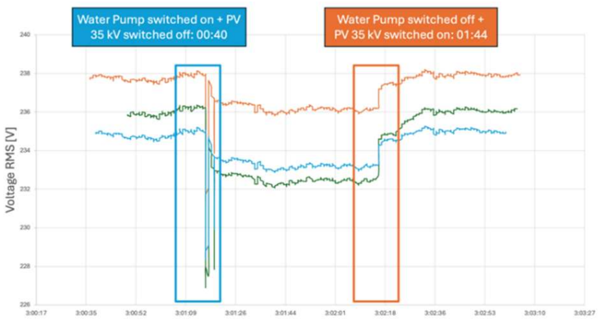

Fig. 2. Measured voltage response to "pump-on + PV-off" event (orange – PV, green – transformer, blue – water pump)

This sag was well within equipment tolerance and did not trigger any undervoltage protection. The BESS inverter reacted almost instantaneously: injection of reactive power was detected, which helped support the voltage, and an uptick in active power output from the BESS compensated for the lost PV generation. As a result, the voltage recovered to within 2–3 % of the nominal value within about 1–2 seconds after the initial dip.

Frequency measurements during the event showed that the microgrid frequency remained relatively stable despite the severe perturbation. In island mode, one might expect a significant frequency drop when a large load such as the pump comes online. However, in this test, the BESS's grid-forming control and the presence of the grid (the PCC was closed to the main grid for safety during initial trials) maintained frequency tightly.

The frequency briefly deviated by only about 0.1 Hz when the pump started and PV tripped, a mild excursion quickly corrected as the BESS and grid support responded. This small frequency deviation indicates that the system possessed sufficient rigidity to handle the abrupt change, thanks in part to fast-response resources. Essentially, the disturbance remained below the threshold that would cause loss of synchronism or large frequency instability.

Throughout the event, all critical parameters stayed within acceptable ranges. Importantly, there were no signs of instability such as sustained oscillations, uncontrollable voltage collapse, or frequency runaway. The system settled to a new steady operating point after the disturbance, and when the PV was reconnected and pump stopped at 01:44, the microgrid smoothly returned to its original state.

Table. I. Key results of the disturbance test

Evaluation parameter	Result
Voltage	8–10% voltage dip
Frequency deviation	~0.1 Hz
BESS response	Active and reactive support
Recovery time	1–2 s
Protection trip	None
Stability assessment	Below estimated RRT

These outcomes confirm that the applied disturbance was within the microgrid's stability margin (i.e., below the RRT). Had the system been near its rigidity limit, we would have observed escalating oscillations or protective trips (for example, the BESS might hit current limits or the frequency might drift outside allowable bounds), forcing test interruption. None of these occurred in our field trial.

D. Data validation of RRT

Using the field data, we performed a post-analysis to quantify how close the disturbance came to the predicted RRT. By feeding the event data (pump power demand profile, PV cutout) into our simulation model, we found that the disturbance magnitude corresponded to roughly 85% of the simulated RRT for that operating scenario. This means the system had a buffer of about 15% in disturbance magnitude before the onset of instability would be expected.

The correspondence between field results and simulation is encouraging, it suggests that the RRT computed via our methods is realistically attainable. Moreover, the field measurement provided insight into dynamic behavior such as the pump's exact inrush characteristic and the PV inverter's dropout response, which can refine the simulation models.

Minor differences were noted (the voltage dip in the field was slightly deeper than in simulation, likely due to the transformer's impedance and unmodeled harmonics, and the recovery took a fraction of a second longer), but these findings are being used to improve the fidelity of the theoretical model.

Overall, the Fót microgrid tests serve as a crucial proof-of-concept that system rigidity and the RRT metric can be observed and validated in practice. The system's ability to withstand the concurrent pump and PV disturbance demonstrates the practical utility of having a unified stability metric: it encapsulates the stress of a multi-faceted event (involving both frequency and voltage aspects) into a single threshold measure.

7. Discussion

The results indicate that system rigidity can serve as a useful composite stability indicator in low-inertia systems. In the Fót microgrid test, the applied disturbance involved both voltage and frequency effects, while the observed response remained within the estimated RRT. At the same time, the measurements showed that the transient voltage dip was the dominant limiting factor in the reported case, whereas the frequency deviation remained small due to the action of the BESS and the support of the main grid.

The simulations also suggest that RRT is sensitive to changes in inertia and control response. Reduced inertia decreases the admissible disturbance level, while fast-acting support such as BESS can increase the stability margin. In this sense, the rigidity metric provides a quantitative way to assess the contribution of synthetic inertia, fast frequency support, and voltage control to overall disturbance tolerance.

Another important aspect is control coordination. The stable response observed during the test indicates that the control actions of the available resources were properly coordinated. This suggests that system rigidity may also be useful for evaluating whether different control layers contribute positively to system stability or introduce adverse interactions.

8. Conclusion

This paper introduced system rigidity and the Rigidity Response Threshold (RRT) as a composite framework for assessing disturbance tolerance in low-inertia power systems. A Lyapunov-based interpretation was used to motivate the concept, while simulation studies and field measurements at the Fót microgrid were used to examine its practical relevance.

The results showed that the tested disturbance remained below the estimated RRT and that the system recovered without instability. In the reported case, the response was primarily limited by voltage dynamics, while frequency remained well controlled due to fast support from the BESS and the grid-connected operating condition. These findings support the use of RRT as a compact indicator of stability margin under the examined conditions.

At the same time, the present validation should be interpreted as a first practical demonstration rather than a complete proof of a universal stability metric. Further work is needed to examine the concept under islanded operation, closer-to-limit disturbances, and larger multi-machine systems. Even so, the results indicate that system rigidity can provide a useful basis for integrated stability assessment in converter-rich, low-inertia networks.

ACKNOWLEDGMENT

This publication was supported by the Bolyai János Research Scholarship of the Hungarian Academy of Sciences (BO/50/24).
Istvan Vokony acknowledge the support of CELSA (eight call) 2023 scholarship.

References

[1]. Kundur, P., Power System Stability and Control, McGraw-Hill, 1994.
[2]. Machowski, J., Bialek, J., Bumby, J., Power System Dynamics: Stability and Control, Wiley, 2020.
[3]. Ulbig, A., Borsche, T., Andersson, G., "Impact of low rotational inertia on power system stability and operation," IFAC Proceedings Volumes, 2014.
[4]. Dörfler, F., Simpson-Porco, J. W., Bullo, F., "Breaking the hierarchy: Distributed control and economic optimality in microgrids," IEEE Transactions on Control of Network Systems, 2016.
[5]. Khalil, H. K., Nonlinear Systems, Prentice Hall, 2002.
[6]. Zhong, Q.-C., Weiss, G., "Synchronverters: Inverters that mimic synchronous generators," IEEE Transactions on Industrial Electronics, 2011.
[7]. Milano, F., Anghel, M., "Impact of time delays on power system stability," IEEE Transactions on Circuits and Systems I, 2012.
[8]. Díaz-González, F. et al., "A review of energy storage technologies for wind power applications," Renewable and Sustainable Energy Reviews, 2012.
[9]. Simpson-Porco, J. W. et al., "Voltage collapse in complex power grids," Nature Communications, 2016.
[10]. Zhang, Y. et al., "Virtual inertia control of power systems with high penetration of renewables: A review," IET Renewable Power Generation, 2018.
[11]. Wang, X., Blaabjerg, F., "Harmonic stability in power electronic-based power systems: Concept, modeling, and analysis," IEEE Transactions on Smart Grid, 2019.
[12]. Milano et al., "Foundations and challenges of low-inertia systems," PSCC, 2018.
[13]. Táczi, I. Vokony, "Review of Stability Analysis in Power Systems with High Penetration of Non-Synchronous Generation," Renew. Energy Power Qual. J., vol. 20, pp. 694–699, Sep. 2022.
[14]. Milano, F., Dörfler, F., Hug, G., Hill, D. J., Verbič, G., "Foundations and challenges of low-inertia systems," Proceedings of the Power Systems Computation Conference (PSCC), 2018.
[15]. Lian, J., Zhang, Y., Ma, C., Yang, H., "Wide-area measurement system-based transient stability assessment considering renewable generation," IEEE Transactions on Power Systems, 2017.
[16]. Gautam, D. et al., "Impact of increased penetration of DFIG-based wind turbine generators on transient and small signal stability of power systems," IEEE Transactions on Power Systems, 2009.
[17]. Fernández-Guillamón, A., Gómez-Lázaro, E., Muljadi, E., Molina-García, Á., "Power systems with high renewable energy sources: A review of inertia and frequency control strategies," Renewable and Sustainable Energy Reviews, 2019.
[18]. Zhou, N., Meng, D., Huang, Z., Welch, G., "Dynamic state estimation of a synchronous machine using PMU data: A comparative study," IEEE Transactions on Smart Grid, 2016.